

Modeling and identification of magnetostrictive hysteresis with a modified rate-independent Prandtl-Ishlinskii model

Wei Wang(王伟), Jun-en Yao(姚骏恩)

Citation: Chin. Phys. B . 2018, 27(9): 098503. **doi:** 10.1088/1674-1056/27/9/098503

Journal homepage: http://cpb.iphy.ac.cn; http://iopscience.iop.org/cpb

What follows is a list of articles you may be interested in

First-order reversal curve investigated magnetization switching in Pd/Co/Pd wedge film

Yan Li(李岩), Wei He(何为), Rui Sun(孙瑞), Zi-Zhao Gong(弓子召), Na Li(李娜), Qeemat Gul, Xiang-Qun Zhang(张向群), Zhao-Hua Cheng(成昭华)

Chin. Phys. B . 2018, 27(4): 047503. **doi:** 10.1088/1674-1056/27/4/047503

Magnetization plateaus and frequency dispersion of hysteresis on frustrated dipolar array

Zhang You-Tian

Chin. Phys. B . 2015, 24(8): 087502. **doi:** 10.1088/1674-1056/24/8/087502

Modelling self-sensing of a magnetostrictive actuator based on a terfenol-D rod

Yan Bai-Ping, Zhang Cheng-Ming, Li Li-Yi, Tang Zhi-Feng, Lü Fu-Zai, Yang Ke-Ji

Chin. Phys. B . 2014, 23(12): 127504. **doi:** 10.1088/1674-1056/23/12/127504

Modeling and identification of magnetostrictive hysteresis with a modified rate-independent Prandtl–Ishlinskii model

Wei Wang(王伟)[1,3] and Jun-en Yao(姚骏恩)[1,2,3,†]

[1] School of Instrumentation Science and Opto-electronics Engineering, Beihang University, Beijing 100083, China
[2] School of Physics and Nuclear Energy Engineering, Beihang University, Beijing 100083, China
[3] Laboratory of Micro-nano Measurement, Manipulation and Physics, Beihang University, Beijing 100083, China

(Received 12 March 2018; revised manuscript received 20 June 2018; published online 28 August 2018)

This paper presents a modified rate-independent Prandtl–Ishlinskii (MRIPI) model based on the Fermi–Dirac distribution for the asymmetric hysteresis description of magnetostrictive actuators. Generally, the classical Prandtl–Ishlinskii (CPI) model can hardly describe the asymmetric hysteresis. To overcome this limitation, various complex operators have been developed to replace the classical operator. In this study, the proposed MRIPI model maintains the classical operator while a modified input function based on the Fermi–Dirac distribution is presented to replace the classical input function. With this method, the MRIPI model can describe the asymmetric hysteresis of magnetostrictive actuators in a relatively simple mathematic format and has fewer parameters to be identified. A velocity-based sine cosine algorithm (VSCA) is also proposed for the parameter identification of the MRIPI model. To verify the validity of the MRIPI model, experiments are performed and the results are compared with those of the existing modeling methods.

Keywords: Prandtl–Ishlinskii model, velocity-based sine cosine algorithm, asymmetric hysteresis nonlinearity, magnetostrictive actuator

PACS: 85.70.Ec, 75.60.–d **DOI:** 10.1088/1674-1056/27/9/098503

1. Introduction

Generally, magnetostriction is the deformation of materials influenced by an external magnetic field. The magnetostrictive effect was first presented by James Joule in 1842,[1] and nowadays the magnetostrictive materials are widely used for micro/nano-level actuation. Due to the characteristics of fast response, high resolution, and high force capacity, magnetostrictive actuators are designed for various applications, such as high speed precision milling machines, hydraulic valves, and active damping systems.[2–4] However, the input–output property of magnetostrictive actuators exhibits considerable hysteresis nonlinearities which deeply reduce their accuracy. Furthermore, their hysteresis curves tend to be asymmetric when driven by moderate or higher amplitude excitations.[5–7]

To address this problem, a number of hysteresis models have been proposed to describe and compensate for the hysteresis of magnetostrictive actuators. The physics-based models are generally derived on the basis of a physical measure, such as magnetization, stress–strain, and energy principles.[8–12] They are usually presented in a complex mathematic format and thus are difficult to invert. Therefore, many phenomenological models, such as Preisach[13–16] and Prandtl–Ishlinskii (P–I) models,[17–20] are proposed. They can be regarded as a superposition of hysteresis operators in relatively simple mathematic formats. Furthermore, P–I models are analytically invertible so that it is convenient to use them to compensate for the hysteresis of magnetostrictive actuators.[18,21,22]

The classical Prandtl–Ishlinskii (CPI) model is composed of a series of classical operators and an input function. Generally, it can only efficiently describe the symmetric hysteresis nonlinearity. To overcome this limitation, much research focuses on the optimization of the classical operators. Therefore, various complex operators have been developed to replace the classical operator. Al Janaideh *et al.* proposed a generalized Prandtl–Ishlinskii (GPI) model established by a superposition of generalized hysteresis operators.[17,22] These generalized operators are formulated by the relatively complex envelope functions, and thus the GPI model can describe the asymmetric and saturated hysteresis properties of different smart actuators. Guanqiao Shan *et al.* studied the hysteresis properties of the voice coil motor experimentally and introduced a modified GPI model to compensate for its asymmetric hysteresis.[23] Kuhnen combined a conventional P–I operator and a dead-zone operator which is used to describe memory-free nonlinearities, and established a new P–I model to describe and compensate for the asymmetric hysteresis of magnetostrictive actuators.[24] These models can describe the asymmetric hysteresis exhibited by magnetostrictive actuators. However, limitations exist in the complex operators when inverting these models mathematically. To balance the modeling performance and model complexity, Guoying Gu *et al.* focused on the optimization of the input function and introduced a modified Prandtl–Ishlinskii (MPI) model by replacing the linear in-

†Corresponding author. E-mail: yaojen@cae.cn

© 2018 Chinese Physical Society and IOP Publishing Ltd

put function with polynomial functions.[18,21] The MPI model only changes the input function and maintains the CPI operator. Therefore, it has a relatively simple mathematic format. More recently, Jinqiang Gan *et al.* added a quadratic polynomial on the basis of the CPI model.[25] This model could describe both rate-independent and rate-dependent hystereses in piezoelectric actuators. Micky Rakotondrabe proposed a multivariable hysteresis model based on the extension of the CPI (monovariable) model.[26] This model avoided the model inversion and could compensate for the hysteresis nonlinearity in a two-degrees-of-freedom (2-DOF) piezoactuator. However, these models have only been verified on piezoceramic actuators and their description of magnetostrictive actuators has not been explored. As illustrated in Ref. [27], all algorithms perform equally on all modeling problems. Therefore, there are still problems that can be solved better by new algorithms. This is the main motivation of this work, in which a new P–I model along with its parameter identification method is proposed for magnetostrictive actuator modeling specifically.

To describe the asymmetric hysteresis phenomenon of magnetostrictive actuators more efficiently, it is necessary to modify the input function for the CPI model. In this paper, a modified rate-independent Prandtl–Ishlinskii (MRIPI) model is introduced for the asymmetric hysteresis description of magnetostrictive actuators. The MRIPI model maintains the classical operator of the CPI model and replaces the linear input function with the Fermi–Dirac distribution. This model has fewer parameters to be identified. Since the MRIPI model only changes the classical input function, it has a relatively simple mathematic format. Compared with the models mentioned above, it is more efficient to establish the MRIPI model and describe the hysteresis phenomenon of magnetostrictive actuators. The properties of this proposed model are characterized. Then the validity of the resulting MRIPI model is demonstrated by comparing the model responses with the measured asymmetric hysteresis of magnetostrictive actuators. Additionally, the performances of the CPI, MPI, GPI, and MRIPI models are compared to analyze the performance of the MRIPI model in describing the asymmetric hysteresis of magnetostrictive actuators. It should be clarified that this study only focuses on the hysteresis independent of the input rate which is called rate-independent hysteresis.

2. MRIPI modeling

Since the proposed MRIPI model is on the basis of the CPI model, before introducing the MRIPI model, the CPI model is reviewed in brief.

2.1. CPI model

The CPI model[15] is a widely accepted phenomenological model. The model is composed of a series of weighted operators and a linear input function. The play operator $F_r[v](t)$, as shown in Fig. 1, is defined by the input $v(t)$ and the threshold r. Assume that $C_{\mathrm{m}}[0,T]$ is the space of the piecewise monotone continuous functions. For any input $v(t) \in C_{\mathrm{m}}[0,T]$, where $0 = t_0 < t_1 < \cdots < t_n = T$ are intervals in $[0,T]$, the output of the play operator $w(t)$ can be described by

$$w(t) = F_r[v](t) = f_r(v(t), w(t_i)) \tag{1}$$

for $t_i < t \le t_{i+1}, 0 \le i \le n-1$, with

$$f_r(v(t), w(t_i)) = \max(v(t) - r, \min(v(t) + r, w(t_i))). \tag{2}$$

The initial value $w(0)$ of the play operator $F_r[v](0)$ can be described by

$$w(0) = F_r[v](0) = f_r(v(0), 0). \tag{3}$$

It has been verified that for any monotone input, the play operator is Lipschitz continuous and monotone.[15] More detailed discussions about this operator are presented in Refs. [15] and [22].

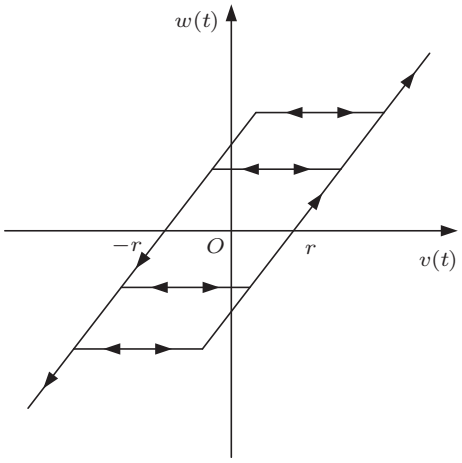


Fig. 1. Input–output relationships of the classical play operator.

The CPI model utilizes a series of weighted operators $F_r[v](t)$ mentioned above to describe the relationship between the input $v(t)$ and the output $w(t)$. The formula of the CPI model $\varphi_{\mathrm{c}}(t)$ can be defined by

$$\varphi_{\mathrm{c}}(t) = p_0 v(t) + \int_0^{\infty} p(r) F_r[v](t) \mathrm{d}r, \tag{4}$$

where p_0 is a positive constant, and $p(r)$ is a positive density function. p_0 and $p(r)$ are generally calculated according to the experimental data. As illustrated in Fig. 2, the CPI model can only describe the symmetric hysteresis nonlinearity efficiently. However, the real hysteresis nonlinearity of magnetostrictive actuators exhibits the asymmetric property, especially when they are driven by moderate or higher amplitude excitations. Therefore, this study proposes an efficient and relatively simple model that can describe the asymmetric hysteresis of magnetostrictive actuators accurately.

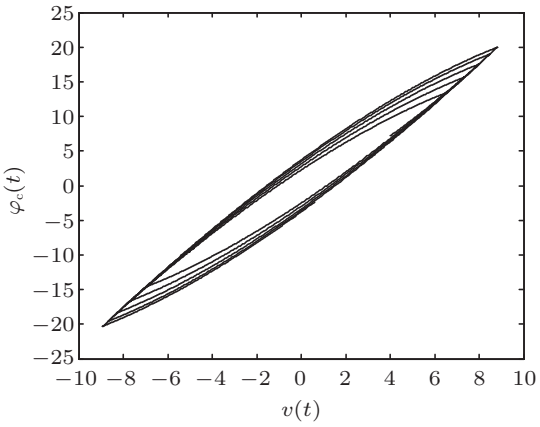


Fig. 2. Hysteresis loops generated by the CPI model with $p_0 = 1.25$, $p(r) = 0.07\mathrm{e}^{-0.1r}$, $r \in [0, 1]$, and the input $v(t) = 5\sin(2\pi t) + 4\cos(6t)$.

2.2. MRIPI model

Considering that the CPI model is devoted to the description of the symmetric hysteresis, a novel MRIPI model based on the Fermi–Dirac distribution is proposed in this study to characterize the asymmetric hysteresis behavior of magnetostrictive actuators. The CPI model is composed of two parts mathematically, a series of weighted operators and a linear input function. The previous proposed models, as mentioned in Section 1, mostly focus on complicating the weighted operators to breakthrough the limitation of the CPI model.[17,22,24] Little research has been conducted on the linear input function. Although Gu *et al.* introduced a MPI model by modifying the linear input function,[18,21] the generalized input function proposed by them has only been verified on piezoceramic actuators. In this study, a simplified Fermi–Dirac distribution is introduced to replace the classical linear input function and the classical operator is maintained. With this method, the MRIPI model can describe the asymmetric hysteresis of magnetostrictive actuators accurately in a relatively simple mathematic format with fewer parameters to be identified.

The hysteresis of magnetostrictive actuators is mainly caused by the magnetization hysteresis of the magnetostrictive materials. It is suggested that the magnetic domains can be described by fermions.[11] Therefore, the Fermi–Dirac distribution can be applied to the magnetic domains. The Fermi–Dirac distribution is usually defined as

$$f(E) = \frac{1}{1 + \mathrm{e}^{\frac{1}{kT}(E - E_\mathrm{F})}}, \tag{5}$$

where $f(E)$ is the probability of a particle having energy E, E_F is the Fermi energy, k is the Boltzmann constant, and T is the absolute temperature. By defining $p = 1/(kT)$ and $q = -E_\mathrm{F}/(kT)$, equation (5) can be rewritten as

$$f(E) = \frac{1}{1 + \mathrm{e}^{pE+q}}. \tag{6}$$

Since the Fermi–Dirac distribution can characterize the properties of the magnetic domains, it is expected to be efficient in magnetization hysteresis description. The proposed MRIPI model replaces the classical linear input function with an extended Fermi–Dirac distribution $g[v](t)$ as follows:

$$g[v](t) = \frac{s}{1 + \mathrm{e}^{pv+q}}, \tag{7}$$

where s is a constant to extend the range of Eq. (6). Therefore, the proposed MRIPI model $\varphi_\mathrm{o}(t)$ is formulated as

$$\varphi_\mathrm{o}(t) = g[v](t) + \int_0^\infty p(r) F_r[v](t)\mathrm{d}r. \tag{8}$$

3. Properties of the MRIPI model

The wiping-out and congruency properties are two basic properties of the operator-based hysteresis models and thus they are essential for the validity of the P–I models.[13,28] According to the Lagrange mean value theorem, the Fermi–Dirac distribution is Lipschitz continuous. Therefore, the proposed MRIPI model fulfills these two properties in theory. The simulations are performed to verified these two properties of the MRIPI model as follows.

3.1. Wiping-out property

The wiping-out property refers to the behavior that any local extremum of the input value wipes out the memory stored by the previous local extrema whose absolute value is smaller than that of the present local extremum.[13–15,28] To exhibit the wiping-out property, a special string sequence $v(t)$ is given as the input of the MRIPI model, as shown in Fig. 3(a). This input string sequence contains six extrema denoted by v_0, v_1, v_2, v_3, v_4, and v_5. Figure 3(b) illustrates the output of the MRIPI model with the input string sequence mentioned above. The density function and the input function of the MRIPI model are $p(r) = 0.07\mathrm{e}^{-0.1r}$ and $g[v](t) = 1/(1 + \mathrm{e}^{-v+2.4})$, respectively. Initially, the input $v(t)$ increases from v_0 to its first maximum v_1, as shown in Fig. 3(a). Accordingly, the output of the MRIPI model $\varphi_\mathrm{o}(t)$ increases from $\varphi_{\mathrm{o}0}$ to $\varphi_{\mathrm{o}1}$ via the curve P_0P_1. Then the input $v(t)$ decreases from v_1 to its first minimum value v_2 and the corresponding output $\varphi_\mathrm{o}(t)$ decreases from $\varphi_{\mathrm{o}1}$ to $\varphi_{\mathrm{o}2}$ via the curve P_1P_2. Subsequently, the input $v(t)$ increases from v_2 to its second maximum v_3. Accordingly, the output $\varphi_\mathrm{o}(t)$ increases from $\varphi_{\mathrm{o}2}$ to $\varphi_{\mathrm{o}3}$ via the lower curve between P_2 and P_3. Since $\varphi_{\mathrm{o}3} < \varphi_{\mathrm{o}1}$, the wiping-out phenomenon does not occur so far. Afterwards, the input $v(t)$ decreases from v_3 to its second minimum value v_4. Since $\varphi_{\mathrm{o}4} < \varphi_{\mathrm{o}3}$, the output $\varphi_\mathrm{o}(t)$ deorbits from the P_2P_3 loop branch and decreases from $\varphi_{\mathrm{o}3}$ to $\varphi_{\mathrm{o}4}$ via the curve $P_3P_2P_4$. In this situation, the memory of $P_2(v_2, \varphi_{\mathrm{o}2})$ is wiped out by the memory of $P_4(v_4, \varphi_{\mathrm{o}4})$. Finally, the input $v(t)$ increases from v_4 to its third maximum v_5. Since $\varphi_{\mathrm{o}5} > \varphi_{\mathrm{o}4}$, the output $\varphi_\mathrm{o}(t)$ deorbits from the $P_1P_2P_4$ loop branch and increases from $\varphi_{\mathrm{o}4}$ to $\varphi_{\mathrm{o}5}$ via the curve $P_4P_1P_5$. Thus the memory of $P_1(v_1, \varphi_{\mathrm{o}1})$ is wiped

out by the memory of $P_5(v_5, \varphi_{o5})$. This simulation shows that the local maximum (minimum) input value will wipe out the memory stored by the previous smaller (larger) local maximum (minimum). Therefore, the wiping-out property of the proposed MRIPI model is verified.

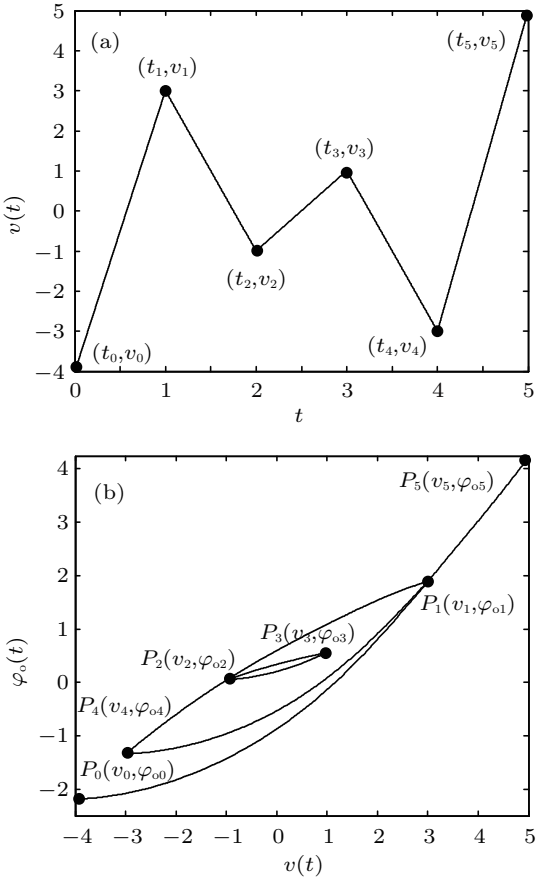


Fig. 3. Simulation of the wiping-out property of the proposed MRIPI model: (a) input current and (b) output hysteresis loops.

3.2. Congruency property

The congruency property refers to that the minor hysteresis loops generated by the same extrema of input are congruent.[13–15,28] To exhibit the congruency property, another special string sequence is given as the input of the MRIPI model, as shown in Fig. 4(a). This input string sequence contains seven extrema denoted by v_0, v_1, v_2, v_3, v_4, v_5, and v_6. On this occasion, assume that v_0 is equal to v_6, v_1 is equal to v_5, and v_2 is equal to v_4. Therefore, the input ranges $[v_2, v_1]$ and $[v_4, v_5]$ are the same. Figure 4(b) illustrates the output of the MRIPI model when the input is the string sequence mentioned above. The density function and the input function of the MRIPI model are the same as those introduced in Subsection 3.1. In Fig. 4(b), the minor hysteresis loop 1 corresponds to the output of the input ranges $[v_2, v_1]$ via first a decreasing then increasing process, and the minor hysteresis loop 2 corresponds to the output of the input ranges $[v_4, v_5]$ via first an increasing then decreasing process. It can be observed that these two minor hysteresis loops are completely congruent. Therefore, the congruency property of the proposed MRIPI model is verified.

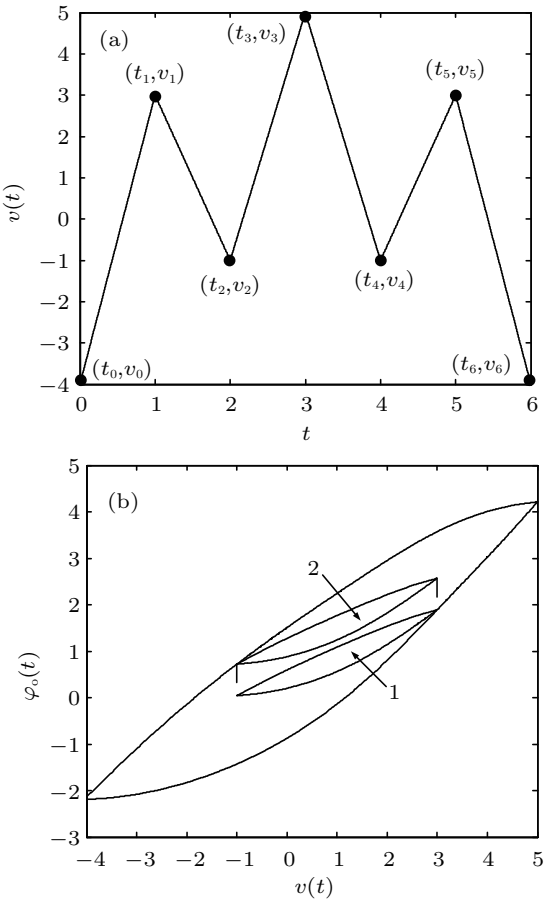


Fig. 4. Simulation of the congruency property of the proposed MRIPI model: (a) input current and (b) output hysteresis loops.

4. Experimental verification

To verify the proposed MRIPI model, the model responses under different amplitudes of excitations are compared with the experimental data in this section. The experimental data of the magnetostrictive actuator analyzed in this paper is reported in Ref. [6] by Subhash Rakheja's group. The input signals are the sinusoidal currents with amplitudes from 1 A to 7 A and a frequency of 10 Hz, and the output displacement exhibits different degrees of asymmetric hysteresis phenomena, as shown in Fig. 5. As reported in Ref. [6], the displacement of the magnetostrictive actuator is nearly symmetric when the amplitude of the input current is lower than 2 A, and the asymmetric phenomena become evident when the amplitude of the input current exceeds 2 A. More detailed information can be found in Ref. [6]. Additionally, the performances of the CPI, MPI, and GPI models are presented and compared with that of the proposed MRIPI model.

In this study, the density function is defined by

$$p(r) = \rho e^{-\tau r}, \tag{9}$$

where ρ is a constant and τ is a positive constant. The threshold function of the classical play operator is defined by

$$r = \alpha j, \quad j = 0,1,2,\ldots,49, \tag{10}$$

where α is the positive constant to be identified by the experimental data. Since the performances of other models are to be presented and compared, the related formulas are introduced briefly as follows. The MPI model only changes the linear input function and maintains the CPI operator. The input function of the MPI model is chosen as $pv^3(t)+qv(t)$, where p and q are constants.[18] The GPI model is formulated by a series of generalized operators with relatively complex envelope functions, and omits the input function. The envelope functions are chosen as $a_i v(t)+b_i$ and $a_i \tanh(b_i v(t)+c_i)+d_i$,[22] respectively. When $i=1$, they are corresponding to the increasing part of the envelope functions. When $i=2$, they are corresponding to the decreasing part of the envelope functions. More detailed information of the MPI model and the GPI model can be found in Refs. [18] and [22].

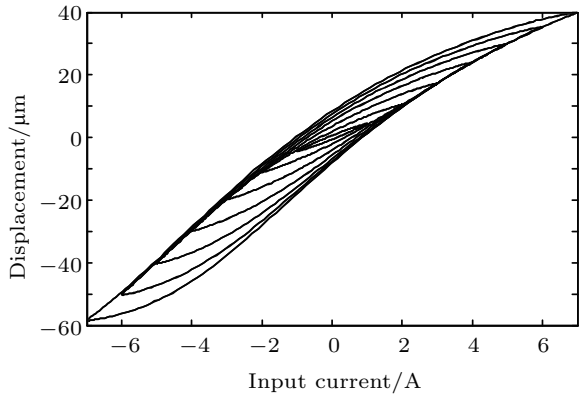


Fig. 5. The experimental data of the magnetostrictive actuator reported in Ref. [6]. The input signals are the sinusoidal currents with amplitudes from 1 A to 7 A and a frequency of 10 Hz.

To experimentally identify the parameters of the MRIPI model, a velocity-based sine cosine algorithm (VSCA) is proposed on the basis of the sine cosine algorithm (SCA).[29] The population-based optimization usually consists of two phases: exploration and exploitation.[30] In the exploration phase, the strategy focuses on widely searching to discover unknown information. However, in the exploitation phase, the strategy aims at finding the optimal solution around a good solution. These two phases must be carefully balanced to avoid slow convergence or local optima stagnation. In the traditional SCA, the position is updated by the following equation:

$$\boldsymbol{X}_i^{t+1} = \begin{cases} \boldsymbol{X}_i^t + r_1 \sin(r_2)\|r_3 \boldsymbol{P}_i^t - \boldsymbol{X}_i^t\|, & r_4 < 0.5, \\ \boldsymbol{X}_i^t + r_1 \sin(r_2)\|r_3 \boldsymbol{P}_i^t - \boldsymbol{X}_i^t\|, & r_4 \geq 0.5, \end{cases} \tag{11}$$

where $\boldsymbol{X}_i^t$ is the position of the current solution in the i-th particle at iteration t, r_1, r_2, and r_3 are random numbers, r_4 is a random number in range [0,1], $\boldsymbol{P}_i^t$ is the position of the destination point in the i-th particle, and $\|\cdot\|$ indicates the absolute value. This equation uses sine and cosine functions to move the particles towards or outwards from the destination randomly. Although the exploration phase is enhanced, its exploitation ability is very poor. In order to improve its exploitation ability, the coefficient of sine and cosine functions in Eq. (11) is usually changed adaptively using the following equation:

$$r_1 = a - t\frac{a}{T}, \tag{12}$$

where t is the current iteration, T is the maximum number of iterations, and a is a constant. Consequently, its convergence is well improved. But since its searching step tends to be shorter due to the change of r_1, the exploitation phase mainly works in the last several iterations and the destination in the beginning iterations cannot be exploited. In this case, even though the result of the exploitation is not satisfying, the particle is unable to jump out of this local optimum and start the exploration again. Since the updating equation is free of the global optimum, there is no guarantee that the global optimum is always found in the last several iterations. Therefore, the exploitation phase probably happens around the local optima. Also the current position of a particle decides its next position directly so that its velocity may change randomly every iteration. This limitation increases the chance to jump over the destination for a particle.

In this study, the VSCA is proposed to improve the exploitation ability of the traditional SCA. In the VSCA, a swarm is composed of m particles. Each particle i is characterized by two vectors: the position vector $\boldsymbol{x}_i = [x_i^1, x_i^2, \ldots, x_i^n]$ and the velocity vector $\boldsymbol{v}_i = [v_i^1, v_i^2, \ldots, v_i^n]$, where n refers to the dimension of the searching space. All the particles are evaluated by the fitness function F as follows:

$$F = \sum_{j=1}^{n} (f_j - y_j)^2, \tag{13}$$

where n is the number of the experimental sampling points, while y_j and f_j are the experimental data and the model output at the jth sampling time, respectively. Comparing the fitness value, each particle records its personal best position as $\boldsymbol{p}_i$, and the global best position as $\boldsymbol{g}$. Then the velocity and position of the ith particle at iteration $t+1$ are updated as

$$\boldsymbol{x}_i^{t+1} = \boldsymbol{x}_i^t + \boldsymbol{v}_i^t, \tag{14}$$

with

$$\boldsymbol{v}_i^{t+1} = \begin{cases} \mu \boldsymbol{v}_i^t + c_1 \sin(\theta)(w_1 \boldsymbol{p}_i - \boldsymbol{x}_i^t) \\ \quad + c_2 \cos(\theta)(w_2 \boldsymbol{g} - \boldsymbol{x}_i^t), & \lambda < 0.5, \\ \mu \boldsymbol{v}_i^t + c_1 \cos(\theta)(w_1 \boldsymbol{p}_i - \boldsymbol{x}_i^t) \\ \quad + c_2 \sin(\theta)(w_2 \boldsymbol{g} - \boldsymbol{x}_i^t), & \lambda \geq 0.5, \end{cases} \tag{15}$$

where c_1 and c_2 are the acceleration coefficients, θ is the direction angle in range $[0,\pi]$, w_1 and w_2 are the inertia weights,

λ is the switch factor in range $[0,1]$, and μ is the friction coefficient expressed by

$$\mu = 0.5 + \frac{\text{rand}}{2}, \tag{16}$$

where rand is a random number between 0 and 1.

To solve the problems of the SCA mentioned above, the VSCA introduces two variables: velocity v and global best value g. The velocity records the change tendency of the distance between the destination and the current position. If the current position is far away from the destination, the velocity will accumulate due to the acceleration during the updating steps. Also the friction factor μ is introduced to avoid overshooting when the particle is already very close to the destination. Therefore, compared with directly updating the position, indirectly updating the position via velocity can improve the searching speed efficiently. To avoid local optima stagnation, the VSCA associates the velocity with the global optimum. Thus, the new position of each particle refers to both the local optima and the global optimum. In this case, when a particle is trapped in a local optimum whose position is far away from that of the global optimum, it will probably jump out of the local optimum, move towards the global optimum, and search along the way again. In the VSCA, there are three states according to the updating equation: accelerating towards the destination, decelerating towards the destination, and decelerating outwards from the destination. When $\theta \in [0, \pi/2]$, the particle accelerates towards the destination rapidly. When $\theta \in (\pi/2, \pi]$ and $\lambda < 0.5$, the particle decelerates towards the destination, where it is either exploiting around the destination or preparing to jump out of the local optima. When $\theta \in (\pi/2, \pi]$ and $\lambda \geq 0.5$, the particle decelerates outwards from the destination, where it is exploring other space out of the current optima space. Thus, the VSCA maintains the exploration ability of the SCA and improves its exploitation ability. Table 1 shows the performances of the VSCA and the SCA. The maximum number of iterations T is 200. The number of particles m is 50, 100, 150, and 200, respectively. The global optimum is around 37 and the local optima are higher than 38. It can be seen that when the number of particles is 50 the VSCA traps in the local optima four times out of ten while the SCA traps six times. As the number of particles increases, the performances of both algorithms are improved. However, the performance of the VSCA is still better than that of the SCA. It should be noted that the VCSA finds the global optimum every time when the number of particles is 200 while the SCA traps in the local optima three times. Therefore, the VSCA is used to identify the MRIPI and other P–I models.

Table 1. Performances of the VSCA and the SCA ($T = 200$). Unit: μm^2

ith	$m = 50$		$m = 100$		$m = 150$		$m = 200$	
	VSCA	SCA	VSCA	SCA	VSCA	SCA	VSCA	SCA
1	36.77	48.12	47.49	47.80	37.94	36.95	36.77	47.15
2	47.78	47.76	36.89	39.21	37.79	46.77	36.76	36.82
3	36.74	36.79	36.76	36.77	36.78	47.78	36.78	40.89
4	40.97	47.75	36.95	46.17	47.45	47.44	36.76	36.80
5	47.72	42.80	47.79	36.81	47.78	36.77	36.84	36.79
6	37.06	37.12	48.22	38.04	36.78	36.78	36.80	36.79
7	36.78	41.99	36.82	36.78	36.78	42.57	36.77	37.12
8	44.79	47.78	36.78	44.43	36.76	36.71	36.78	41.57
9	36.78	36.77	38.07	47.71	36.77	39.42	36.74	36.78
10	36.72	36.79	36.78	36.78	36.77	36.76	36.77	36.75
Average	40.21	42.37	40.25	41.15	39.16	40.79	36.78	38.75
Standard deviation	4.77	5.18	5.25	4.99	4.48	4.87	0.03	3.48

Figure 6 illustrates the performances of the CPI model and the MRIPI model when the amplitudes of the input current are 1 A, 3 A, 5 A, and 7 A. In Fig. 6(a), it can be observed that the outputs of the CPI model match with the experimental data quite well when the amplitude of the input current is 1 A. However, it generates relatively large deviations, especially at both ends of the hysteresis loop, when the amplitudes of the input current exceed 3 A. Figure 6(b) shows the performance of the proposed MRIPI model under different amplitudes of excitations. It can be observed that the model matches with all the experimental data quite well. To quantify the performances of these models, the relative root-mean-square error e_{rms} is calculated by

$$e_{\text{rms}} = \frac{\sqrt{\frac{1}{n}\sum_{i=1}^{n}(y_i - f_i)^2}}{\max_i(y_i) - \min_i(y_i)}, \tag{17}$$

and the relative maximum error $e_{\max}$ is calculated by

$$e_{\max} = \frac{\max_i |y_i - f_i|}{\max_i(y_i) - \min_i(y_i)}. \tag{18}$$

Figure 7 illustrates the comparison of e_{rms} and $e_{\max}$ between

the MRIPI model and the CPI model. In Fig. 7, it can be observed that as the amplitude of the input current increases from 1 A to 7 A, $e_{\rm rms}$ of the MRIPI model stays less than 1% and $e_{\rm max}$ of the MRIPI model stays less than 2% while those of the CPI model continuously increase.

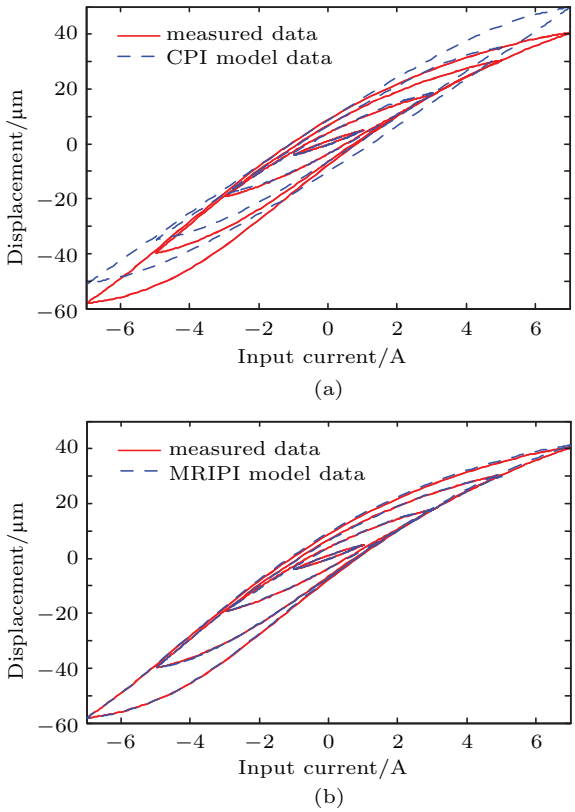


Fig. 6. (color online) Performances of (a) CPI model and (b) MRIPI model when the amplitudes of the input current are 1 A, 3 A, 5 A, and 7 A.

To further analyze the performance of the MRIPI model, the outputs of the MPI model and the GPI model are presented and compared with those of the MRIPI model. The input signal is the sinusoidal current with an amplitude of 3 A and a frequency of 10 Hz. In Fig. 8(a), it can be observed that the output of the MRIPI model matches with the experimental data quite well. Figure 8(b) shows that although the MPI model can describe the asymmetric hysteresis behavior of piezoceramic actuators, it is difficult to describe the asymmetric hysteresis behavior of magnetostrictive actuators. The possible reason is that the asymmetric hysteresis loop of magnetostrictive actuators exhibits evident saturation on both ends. The GPI model is proposed to describe the asymmetric hysteresis behavior of smart actuators, including magnetostrictive actuators. The outputs of the GPI models with different envelope functions are illustrated in Figs. 8(c) and 8(d), respectively. The GPI model 1 has linear envelope functions as mentioned at the beginning of this section. This model can describe the asymmetric hysteresis behavior without saturation. Since it is reported that the output saturation becomes evident when the input current exceeds 2 A,[6] the performance of the GPI model 1 is limited in describing the asymmetric hysteresis behavior of magnetostrictive actuators driven by moderate or higher amplitude excitations. Therefore, the GPI model 2 with hyperbolic tangent envelope functions mentioned at the beginning of this section is proposed. It is observed that the output of this model matches the experimental data very well. However, compared with the proposed MRIPI model, this model has a relatively complex mathematic format with more parameters to identify.

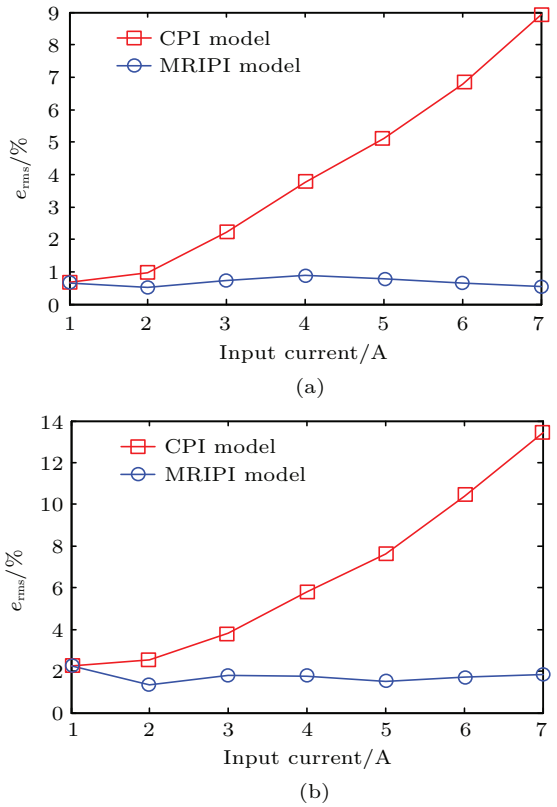


Fig. 7. (color online) Comparison of prediction errors, (a) the relative root-mean-square error $e_{\rm rms}$ and (b) the relative maximum error $e_{\rm max}$, between the MRIPI model and the CPI model as the amplitudes of the input current increase from 1 A to 7 A.

Table 2 lists the parameter number to be identified, the relative root-mean-square error $e_{\rm rms}$, and the relative maximum error $e_{\rm max}$ of these four P–I models. The detailed parameter values are listed in Table 3. It can be seen that to achieve low errors there are fewer parameters to be identified for the MRIPI model, and thus the efficiency of the modeling process is improved. Although the parameter number of the MPI model is one less than that of the MRIPI model, the performance of the MRIPI model is much better than that of the MPI model. The smaller $e_{\rm rms}$ and $e_{\rm max}$ of the MRIPI model indicate that the proposed model has a better description of both the global and local characteristics of the asymmetric hysteresis behavior exhibited by magnetostrictive actuators. In conclusion, the proposed MRIPI model can well describe the asymmetric hysteresis behavior of magnetostrictive actuators in a relatively simple mathematic format.

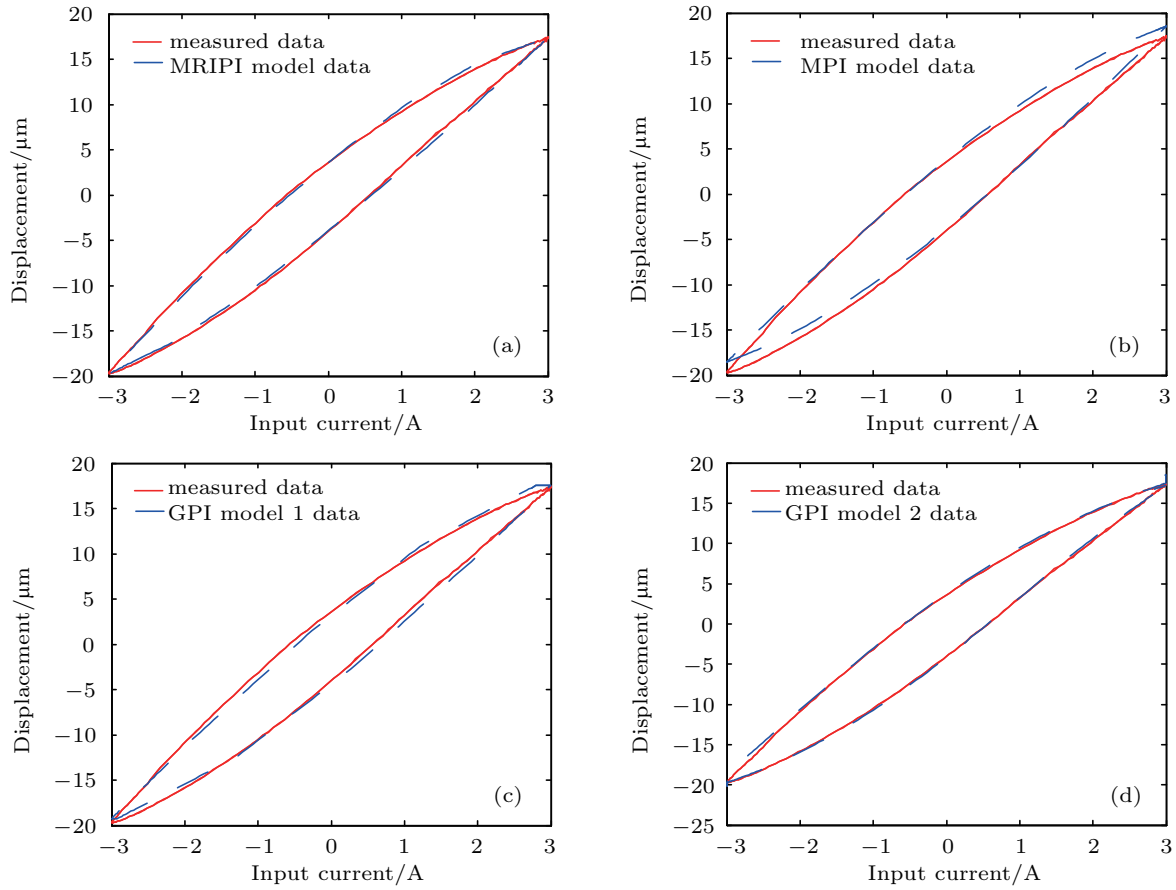


Fig. 8. (color online) Experimental verification of the MRIPI model with a sinusoidal input current and comparisons between the MRIPI model and other common P–I models: (a) MRIPI model data, (b) MPI model data, (c) data of the GPI model 1 with linear envelope functions, and (d) data of the GPI model 2 with hyperbolic tangent envelope functions. The amplitude of the input current is 3 A and the frequency is 10 Hz.

Table 2. Performances of the P–I models.

	MRIPI model	MPI model	GPI model 1	GPI model 2
Parameters	6	5	7	11
$e_{\rm rms}/\%$	0.71	2.18	1.19	0.70
$e_{\rm max}/\%$	1.77	3.70	2.33	3.38

Table 3. Parameters of the P–I models.

Parameter	MRIPI model	MPI model	GPI model 1	GPI model 2
α	0.47	0.06	3.83	6.95
ρ	2.81	2.21	0.87	1.72
τ	0.95	0.32	0.18	0.09
s	–4.8976	–	–	–
p	1.05	0.02	–	–
q	3.19	2.40	–	–
a_1	–	–	4.78	12.27
b_1	–	–	-0.69	0.33
c_1	–	–	–	–0.02
d_1	–	–	–	–0.43
a_2	–	–	4.88	16.41
b_2	–	–	-0.03	0.24
c_2	–	–	–	0.27
d_2	–	–	–	–3.19

5. Conclusion

The proposed modified classical Prandtl–Ishlinskii model identified by the VSCA can accurately characterize the asymmetric hysteresis behavior of magnetostrictive actuators. The performance of the MRIPI model is stable under different amplitudes of applied current. The relative root-mean-square error stays less than 1% and the relative maximum error stays less than 2% when the amplitudes of the input current increase from 1 A to 7 A. Compared with the classical Prandtl–Ishlinskii model, the proposed model has a better description of both the local and global asymmetric hysteresis behaviors exhibited by magnetostrictive actuators. Additionally, the proposed model has a relatively simple mathematic format with fewer parameters to be identified. Thus, it is more efficient to establish the MRIPI model and describe the asymmetric hysteresis phenomenon of magnetostrictive actuators. The performances of different Prandtl–Ishlinskii models are also compared to show better accuracies of the proposed model. The inverse model of the MRIPI model will be studied and the compensator control method of magnetostrictive actuators will be designed in the future.

Acknowledgment

The authors wish to thank Prof. Subhash Rakheja, Prof. Mohammad Al Janaideh, and Prof. Omar Aljanaideh for providing their experimental data of magnetostrictive actuators.

References

[1] Joule J P 1847 *Philosophical Magazine Series 3* **30** 76
[2] Olabi A G and Grunwald A 2008 *Materials and Design* **29** 469
[3] Oates W S and Smith R C 2008 *Journal of Inteltigent Material Systems and Structures* **19** 193
[4] Karunanidhi S and Singaperumal M 2010 *Sensors and Actuators A: Physical* **157** 185
[5] Calkins F T, Smith R C and Flatau A B 2000 *IEEE Transactions on Magnetics* **36** 429
[6] Aljanaideh O, Rakheja S and Su C Y 2014 *Smart Materials and Structures* **23** 35002
[7] Dapino M J, Smith R C and Flatau A B 2000 *IEEE Transactions on Magnetics* **36** 545
[8] Ikuta K, Tsukamoto M and Hirose S 1991 *Proceedings of Micro Electro Mechanical Systems* January 30, 1991, Nara, Japan, p. 103
[9] Smith R C, Seelecke S, Ounaies Z and Smith J 2003 *Journal of Intelligent Material Systems and Structures* **14** 719
[10] Smith R C and Ounaies Z 2000 *Journal of Intelligent Material Systems and Structures* **11** 62
[11] Liu C 2015 *Computational Materials Science* **110** 295
[12] Liu Q Y, Luo X, Zhu H Y, Han Y W and Liu J X 2017 *Acta Phys. Sin.* **66** 107501 (in Chinese)
[13] Mayergoyz I 1986 *IEEE Transactions on Magnetics* **22** 603
[14] Macki J W, Nistri P and Zecca P 1993 *Siam Review* **35** 94
[15] Brokate M and Sprekels J 1996 *Hysteresis and Phase Transitions* (Berlin: Springer) pp. 80–85
[16] Mittal S and Menq C H 2000 *IEEE/ASME Transactions on Mechatronics* **5** 394
[17] Al Janaideh M, Rakheja S and Su C Y 2009 *Smart Materials and Structures* **18** 3149
[18] Gu G Y, Zhu L M and Su C Y 2014 *IEEE Transactions on Industrial Electronics* **61** 1583
[19] Yang M J, Li C X, Gu G Y and Zhu L M 2015 *Smart Materials and Structures* **24** 125006
[20] Yu Z, Liu Y, Wang Y, Li S and Tan J 2017 *Chinese Journal of Scientific Instrument* **38** 129 (in Chinese)
[21] Gu G Y, Yang M J and Zhu L M 2012 *Review of Scientific Instruments* **83** 065106
[22] Al Janaideh M, Rakheja S and Su C Y 2011 *IEEE/ASME Transactions on Mechatronics* **16** 734
[23] Shan G, Li Y, Zhang Y, Wang Z and Qian J 2016 *Sensors and Actuators A: Physical* **251** 10
[24] Kuhnen K 2003 *European Journal of Control* **9** 407
[25] Gan J, Zhang X and Wu H 2016 *Review of Scientific Instruments* **87** 035002
[26] Rakotondrabe M 2017 *Nonlinear Dynamics* **89** 481
[27] Wolpert D H and Macready W G 1997 *IEEE Transactions on Evolutionary Computation* **1** 67
[28] Liu S and Su C Y 2011 *Smart Materials and Structures* **20** 225
[29] Mirjalili S 2016 *Knowledge-Based Systems* **96** 120
[30] Črepinšek M, Liu S H and Mernik M 2013 *ACM Computing Surveys (CSUR)* **45** 35